International Journal of Bifurcation and Chaos, Vol. 25, No. 2 (2015) 1550033 (7 pages)

DOI: 10.1142/S0218127415500339

New Chaotic Regimes in the Lorenz and Chen Systems

J. C. Sprott
Department of Physics, University of Wisconsin,
Madison, Wisconsin 53706, USA
sprott@physics.wisc.edu

Received November 10, 2014

It has recently been shown that the Chen system with $c > 0$ is identical to the reversed-time Lorenz system with particular negative parameters and that the Chen system with $c < 0$ is identical to the forward-time Lorenz system with particular negative parameters. This note describes this new regime and shows that it admits chaotic solutions that were previously unexplored in either system.

Keywords: Chaos; symmetry; attractor.

1. Introduction

The Lorenz system [Lorenz, 1963] given by

$$\begin{aligned}\dot{X} &= \sigma(Y - X)\\ \dot{Y} &= \rho X - Y - XZ\\ \dot{Z} &= -\beta Z + XY\end{aligned} \tag{1}$$

has long been a paradigm of chaos since it has strange attractors over a significant range of the parameters (σ, ρ, β) usually taken to be positive with typical values of $(10, 28, 8/3)$. Similarly, the Chen system [Chen & Ueta, 1999] given by

$$\begin{aligned}\dot{x} &= a(y - x)\\ \dot{y} &= (c - a)x + cy - xz\\ \dot{z} &= -bz + xy\end{aligned} \tag{2}$$

has been much studied for positive values of its parameters (a, b, c) and has chaotic solutions for typical parameters of $(35, 3, 28)$.

Recently, Algaba *et al.* [2013] have shown that the Chen system has only two independent parameters a/c and b/c and that it is identical to the reversed-time Lorenz system for $c > 0$ and to the forward-time Lorenz system for $c < 0$ in the parameter plane $\rho + \sigma = -1$. Hence it follows that the Lorenz system has a strange repeller for certain negative values of its parameters corresponding to the strange attractor in the Chen system with certain positive parameters. Furthermore, Algaba *et al.* showed that for $c < 0$, Chen's attractor exists if the Lorenz attractor exists in this unusual range of its parameters. In particular, for $c = -1$ the two equations are identical provided $\sigma = a, \rho = c - a$, and $\beta = b$. The purpose of this paper is to show that such attractors do exist and to determine their properties and the conditions under which they occur.

2. Parameter Space of the Chen System

Since the Chen system has only two independent parameters, it is feasible to explore its entire parameter space and identify all possible dynamical behaviors. This would be more difficult for the Lorenz system since it has three parameters. It is worth noting that since Eq. (2) has seven terms, four of whose coefficients can be set to unity by a linear rescaling of x, y, z, and t, its most general form would have an additional parameter that has been implicitly set to 1.0 and that could be introduced to make an even stronger connection to the Lorenz

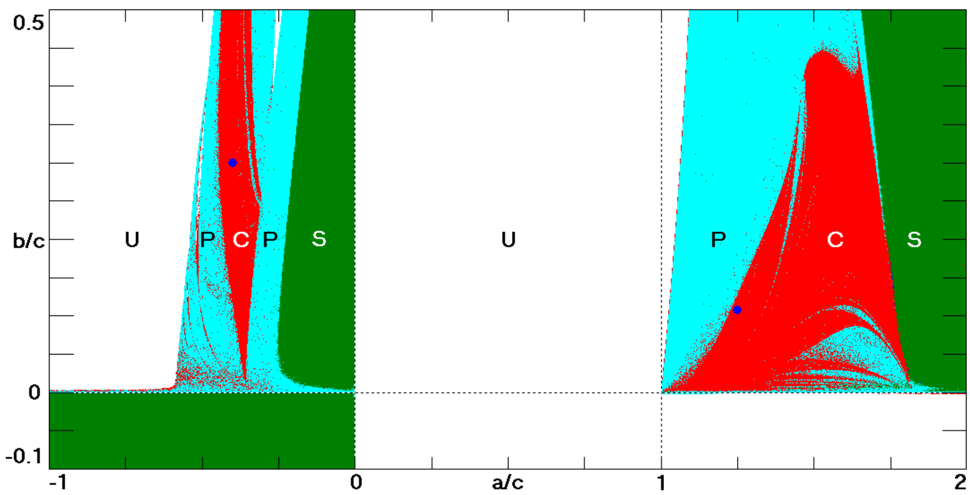

Fig. 1. Dynamical regions of the Chen system over its entire parameter range; U = unbounded, P = periodic, C = chaotic, S = stable.

system. In particular, if the factor $(c-a)$ in Eq. (2) were replaced with a new independent parameter ρ, Eq. (2) would become functionally identical to the Lorenz system (1) for $c=-1$.

Figure 1 shows all the dynamical regions in the parameter space of the Chen system for all signs of the parameters. Most solutions are unbounded, but there are two distinct regions that admit attractors, one for positive c and the other for negative c. For each point in this plot, it was necessary to search for initial conditions that give bounded solutions and then to estimate the largest Lyapunov exponent for each point. The criterion used was to assume that Lyapunov exponents in the range $(-0.001, 0.001)$ are periodic (limit cycles), those that are more negative are stable equilibria (point attractors), and those that are more positive are chaotic (strange attractors), shown in their respective colors.

The absence of attractors at intermediate values of a/c is easily understood by noting that the rate of volume expansion for Eq. (2) is given by $-a+c-b$, which is positive for $0 < a/c < 1-b/c$. The case with $c=0$ is a special case of the "T-system" [Tigan & Opriş, 2008; Jiang *et al.*, 2010] with a single parameter b/a, and it is not equivalent to the Lorenz system for any choice of parameters. For $b/a < -1$ and $c=0$, the system is volume-expanding, and all solutions are unbounded. For $-1 < b/a < 0$ and $c=0$, all solutions approach infinity along the $+z$ axis. For $b/a > 0$ and $c=0$, all solutions approach a stable equilibrium at the origin. Hence, there are no periodic or chaotic solutions for $c=0$. Note also that no attractors exist for $b/c < 0$ when $a/c > 0$.

The region in the upper right quadrant of Fig. 1 is the conventional Chen system with positive parameters that has been much studied [Ueta & Chen, 2000; Lü *et al.*, 2002], with the usual parameters shown as a blue dot, and thus will not be further examined here. The region on the left is the new regime that admits chaotic solutions, not previously observed. It maps into the forward-time Lorenz system provided the parameters are chosen according to $\sigma = -a/c, \rho = a/c - 1, \beta = -b/c$, which is a seldom considered region of the Lorenz system. Some special cases of the Lorenz system with negative and zero parameters have been studied [Čelikovský & Vaněček, 1994; Čelikovský & Chen, 2002, 2005; Cao & Zhang, 2007; Llibre *et al.*, 2010; Sprott, 2010; Li & Sprott, 2014], but apparently not the one considered here.

3. Equilibria

The starting point for analysis of system (2) is to identify the equilibria with $c < 0$ and their properties. One equilibrium is at $(x^*, y^*, z^*) = (0,0,0)$ with eigenvalues that satisfy $\lambda^3 + (a+b-c)\lambda^2 + (ab - bc - 2ac + a^2)\lambda + ab(a-2c) = 0$. For $0 > a/c > -0.1547$ this equilibrium is a node, and for $a/c < -0.1547$ it is a focus. For $b/c < 0$ the equilibrium is stable, and for $b/c > 0$ it is unstable. This accounts for the stable region in Fig. 1 for $b/c < 0$ and allows us to focus on the region $b/c > 0$ where the equilibrium at the origin is unstable and chaos can occur.

The other two equilibria are at $(\pm x^*, \pm y^*, z^*)$ where $x^* = y^* = \sqrt{b(2c-a)}$ and $z^* = 2c - a$ with eigenvalues that satisfy $\lambda^3 + (a + b - c)\lambda^2 + bc\lambda + 2ab(2c - a) = 0$. These equilibria experience a supercritical Hopf bifurcation when $\lambda = i\omega$, giving birth to limit cycles with a frequency $\omega = \sqrt{bc}$, and this occurs along the curve given by $\frac{b}{c} = 1 + \frac{a}{c}(3 - 2\frac{a}{c})$, which coincides with the upper part of the boundary between the periodic and stable regions on the left in Fig. 1.

4. Bifurcations

To continue the bifurcation analysis, it suffices to consider a one-dimensional variation of a/c at a fixed value of $b/c = 0.3$, which cuts across the various dynamical regions shown in Fig. 1. Figure 2 shows the Lyapunov exponents, Kaplan–Yorke dimension and bifurcation diagram starting on the right from the stable equilibria, and continuing to the Hopf bifurcation at $a/c = 0.75 - \sqrt{0.9125} = -0.20525$ where a symmetric pair of limit cycles is born. The limit cycles grow in size until a new symmetric limit cycle is born at infinity for $a/c \approx -0.284$ and begins shrinking, and the three limit cycles coexist until $a/c \approx -0.297$ where the two symmetric limit cycles disappear. The larger symmetric limit cycle remains until $a/c \approx -0.309$ where its symmetry breaks in a pitchfork bifurcation, forming a symmetric pair of interlinked limit cycles. These limit cycles then begin period doubling at $a/c \approx -0.319$ and form a symmetric pair of strange attractors at $a/c \approx -0.322$. These strange attractors grow in size until they merge into a single symmetric strange attractor at $a/c \approx -0.325$.

The chaos persists except for periodic windows until $a/c \approx -0.4208$ where a bifurcation occurs with a symmetric pair of heteroclinic orbits that connect the symmetric saddle foci as shown in Fig. 3. Since the eigenvalues for these equilibria are given by $-1.2654197, 0.0723099 \pm 0.6912134i$, the Shilnikov condition [Shilnikov *et al.*, 2001] for the existence of chaos is satisfied. For $a/c < -0.4208$, there is

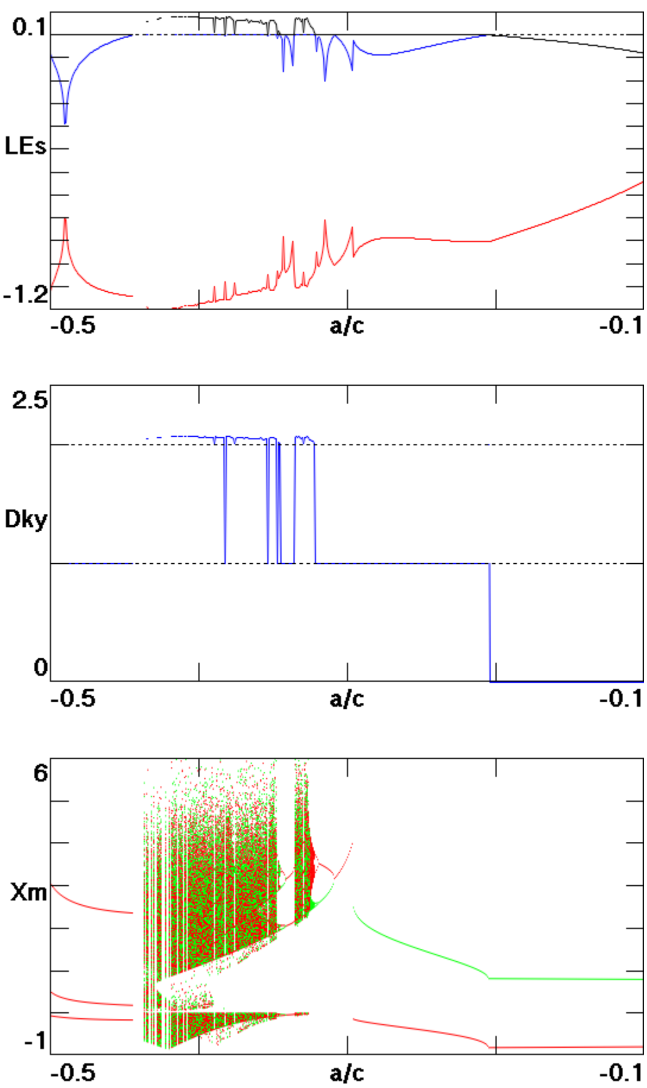

Fig. 2. Lyapunov exponents (LEs), Kaplan–Yorke dimension (Dky), and maximum values of x (Xm) versus a/c with $(b, c) = (-0.3, -1)$ in Eq. (2). The plot of Xm shows the maxima of x in green and the negative of the minimum of x in red so as to distinguish the symmetric and nonsymmetric solutions.

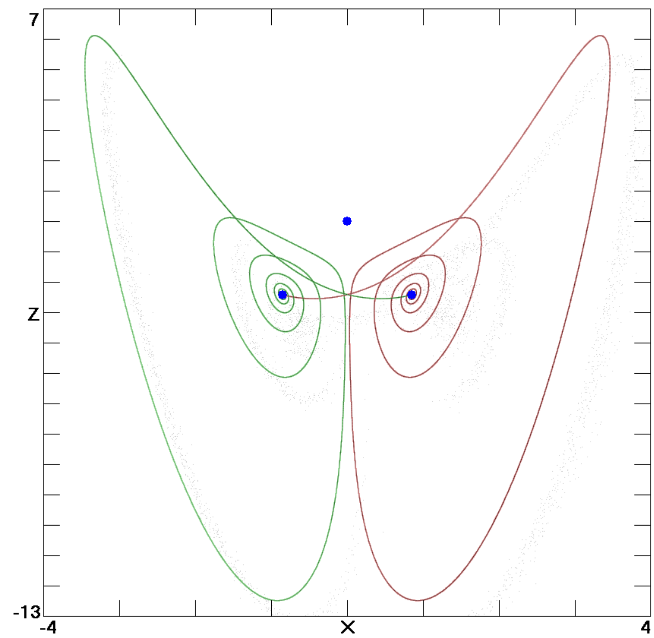

Fig. 3. Projection onto the xz-plane of the double heteroclinic orbits for $(a, b, c) = (0.4208, -0.3, -1)$ with initial conditions $(x_0, y_0, z_0) = (\pm 0.8522, \pm 0.8519, -2.421)$ in Eq. (2).

a region of long duration chaotic transients and unbounded orbits, until a new symmetric limit cycle appears in the approximate range $-0.444 > a/c > -0.518$. For $a/c < -0.518$, all orbits are unbounded. All the behavior described here also occurs in the Lorenz system provided $\sigma = -a/c$, $\rho = a/c - 1$, and $\beta = -0.3$.

5. Attractors

The behavior just described gives rise to a variety of attractors including stable equilibria, limit cycles, and strange attractors, some of which are shown in Fig. 4. For $a/c = -0.29$, a symmetric pair of limit cycles coexist with a larger symmetric limit cycle.

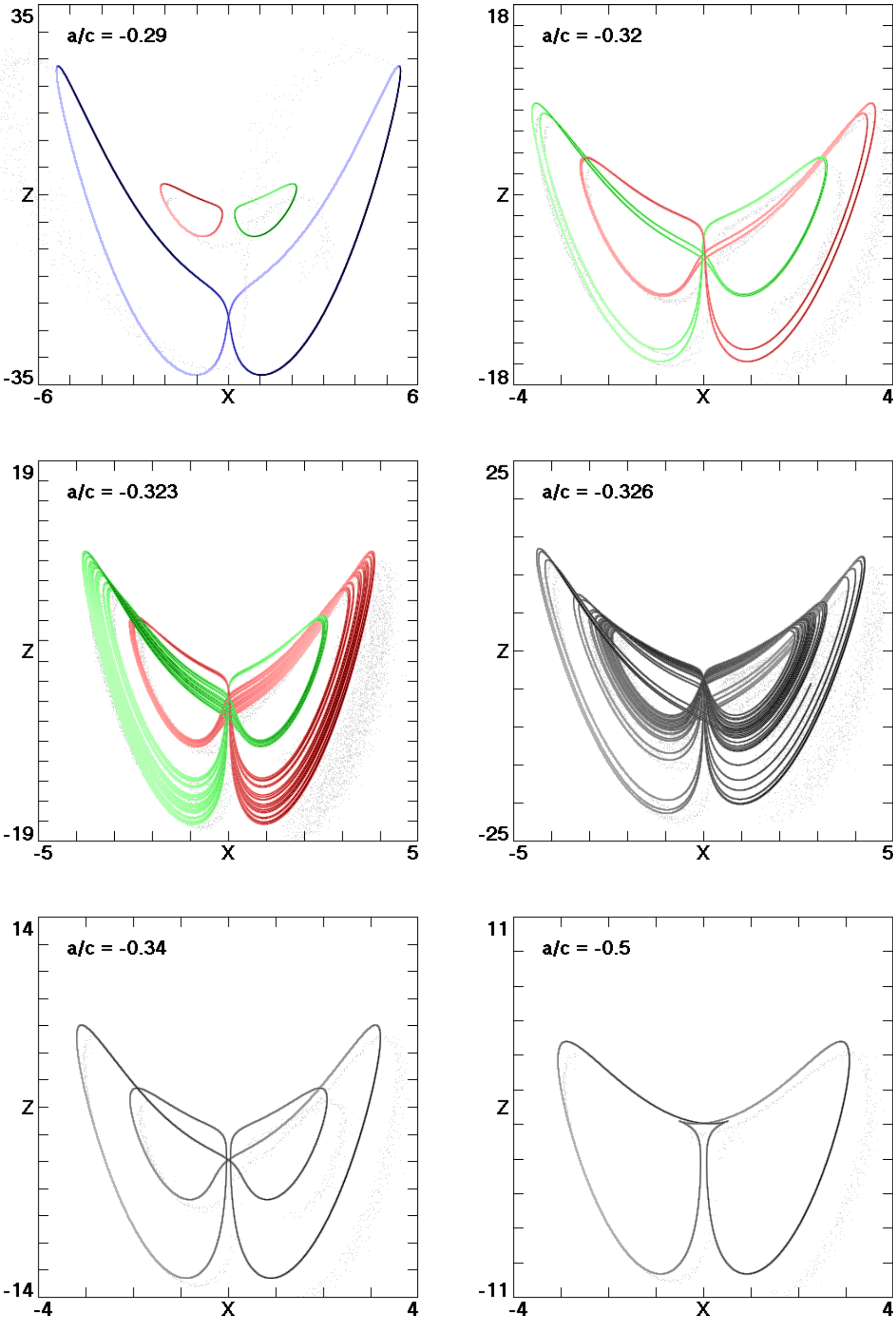

Fig. 4. Various attractors for Eq. (2) with $b = -0.3$ and $c = -1$ for different values of a/c projected onto the xz-plane.

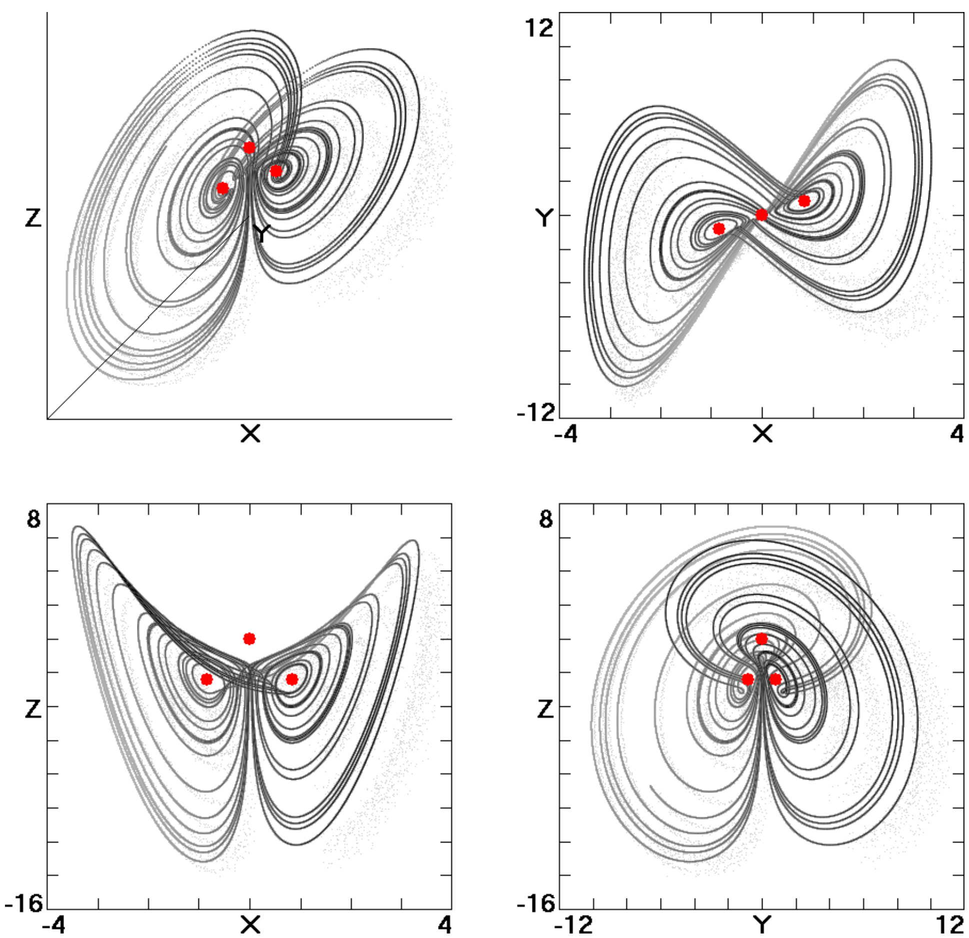

Fig. 5. Four views of the strange attractor for $(a, b, c) = (0.4, -0.3, -1)$ with initial conditions $(x_0, y_0, z_0) = (1, 0, 0)$ in Eq. (2). The three equilibrium points are shown as red dots.

For $a/c = -0.32$, a symmetric pair of period-2 limit cycles are interlocked. For $a/c = -0.323$, a symmetric pair of strange attractors are interlocked. For $a/c = -0.326$, the symmetric pair of strange attractors has merged into a single symmetric strange attractor. For $a/c = -0.34$, there is a window with a symmetric period-2 limit cycle. For $a/c = -0.5$ there is a symmetric limit cycle.

Figure 5 shows a more detailed view of the strange attractor that occurs toward the middle of the chaotic region at $(a, b, c) = (0.4, -0.3, -1)$ as shown by a blue dot on the left side of Fig. 1. For this case, the Lyapunov exponents are $(0.0743, 0, -1.1743)$, and the Kaplan–Yorke dimension is 2.0633. The same attractor occurs for the Lorenz system in Eq. (1) with $(\sigma, \rho, \beta) = (0.4, -1.4, -0.3)$.

6. Basin of Attraction

The Lorenz system with positive parameters is globally attracting except for the three equilibrium points as can be understood intuitively by noting that all three of the equations in Eq. (1) are damped. Similarly, the Chen system with the usual positive parameters is also globally attracting [Ueta & Chen, 2000] despite the antidamping term cy in Eq. (2). However, the Chen system with $c < 0$ in the chaotic regime and its Lorenz counterpart, also with two damping terms and one antidamping term in the $\dot{z}$ and $\dot{Z}$ equations, do not have global attractors.

Figure 6 shows in light blue a cross-section of the basin of attraction in the plane $z = -2.4$ for the strange attractor in Fig. 5. This is the plane in which the symmetric saddle points lie, as indicated by the red dots in the figure. Also shown in black is a cross-section of the strange attractor. The white regions of the plot correspond to initial conditions that approach infinity as $t \to \infty$. Plots in other planes that intersect the attractor are similar. Since the equilibrium points are completely surrounded by the basin of the strange attractor, it is

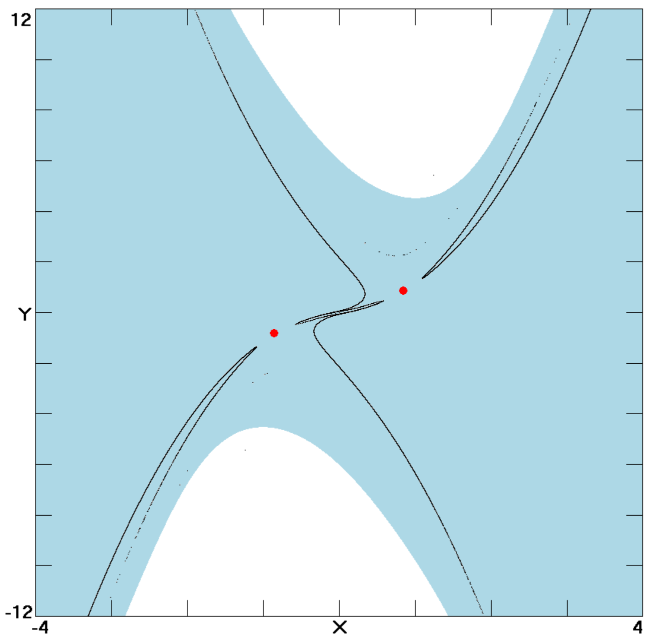

Fig. 6. Cross-section of the strange attractor (black) and its basin of attraction (light blue) in the plane $z = -2.4$ for $(a, b, c) = (0.4, -0.3, -1)$ in Eq. (2). The two saddle points that lie in the plane are shown as red dots.

an example of a self-excited attractor [Leonov & Kuznetsov, 2013].

It is useful to quantify the size of a basin of attraction, but this is difficult because some basins have infinite volume but occupy a negligible fraction of the state space, while others have finite volume yet stretch to infinity in certain directions. Furthermore, the basin boundary may be a fractal. A proposed method proceeds as follows.

First find the center of mass of the attractor by averaging each of its variables over time and the standard deviation of the distance of the orbit from that center as a measure of the size of the attractor. Then construct (hyper)spheres of various sizes centered on the center of mass, for example using radii of $r = 1, 2, 4, 8, \ldots$ standard deviations. Then in Monte Carlo style, pick random initial conditions uniformly distributed inside the spheres, and calculate the probability P that the points are in the basin of attraction. Then make a plot of $\log(P)$ versus $\log(r)$. In the limit $r \to \infty$, the curve will typically be straight with a slope γ such that $P(r) = (r_0/r)^\gamma$ where γ is the codimension of the basin (the dimension of the space not in the basin) and r_0 is a measure of its linear size relative to the attractor if $\gamma > 1$. For $\gamma < 1$, $P(r)$ gives an estimate of the probability that a point within a distance r from the center of the attractor is within its basin.

This method was applied to the strange attractor in Fig. 5 whose center is at $(x_c, y_c, z_c) \approx (0, 0, -3.1875)$ and whose size is

$$\sqrt{\langle (x - x_c)^2 + (y - y_c)^2 + (z - z_c)^2 \rangle} \approx 3.7288.$$

Over the range $0 \le \log_2(r) \le 10$, a least squares fit of $\log(P)$ versus $\log(r)$ gives $\gamma \approx 0.01$, which is not convincingly different from zero. Thus $P(r)$ is nearly constant over the range with an average value of about 0.86, which is suspiciously close to what would be expected if all but one of the eight octants in state space lies in the basin ($7/8 = 0.875$). However, initial conditions that lie outside the basin are scattered among all eight octants, although they all escape in the $-z$ direction. Therefore, unlike the conventional Chen attractor with $c > 0$, this one with $c < 0$ is not globally attracting, but suitable initial conditions are easily found.

7. Conclusions

The dynamical behavior of the Chen system has been examined throughout its entire two-dimensional parameter space with special attention to the region with $c < 0$ where it maps into the Lorenz system with negative parameters. This new regime admits stable equilibria, coexisting limit cycles, symmetry breaking, period-doubling, chaos, attractor merging, and heteroclinic orbits satisfying the Shilnikov condition for the existence of chaos.

Acknowledgment

I am grateful to Xiong Wang and Nikolay Kuznetsov for helpful discussions.

References

Algaba, A., Fernández-Sánchez, F., Merino, M. & Rodríguez-Luis, A. J. [2013] "Chen's attractor exists if Lorenz repulsor exists: The Chen system is a special case of the Lorenz system," *Chaos* **23**, 033108-1–6.

Cao, J. & Zhang, X. [2007] "Dynamics of the Lorenz system having an invariant algebraic surface," *J. Math. Phys.* **48**, 1–13.

Čelikovský, S. & Vaněček, A. [1994] "Bilinear systems and chaos," *Kybernetika* **30**, 403–424.

Čelikovský, S. & Chen, G. [2002] "On a generalized Lorenz canonical form of chaotic systems," *Int. J. Bifurcation and Chaos* **12**, 1789–1812.

Čelikovský, S. & Chen, G. [2005] "On the generalized Lorenz canonical form," *Chaos Solit. Fract.* **26**, 1271–1276.

Chen, G. & Ueta, T. [1999] "Yet another chaotic attractor," *Int. J. Bifurcation and Chaos* **9**, 1465–1466.

Jiang, B., Han, X. & Bi, Q. [2010] "Hopf bifurcation analysis in the T-system," *Nonlin. Anal.*: *Real World Appl.* **11**, 522–527.

Leonov, G. A. & Kuznetsov, N. V. [2013] "Hidden attractors in dynamical systems. From hidden oscillations in Hilbert–Kolmogorov, Aizerman, and Kalman problems to hidden chaotic attractor in Chua circuits," *Int. J. Bifurcation and Chaos* **23**, 1330002-1–69.

Li, C. & Sprott, J. C. [2014] "Multistability in the Lorenz system: A broken butterfly," *Int. J. Bifurcation and Chaos* **24**, 1450131-1–7.

Llibre, J., Messias, M. & da Silva, P. R. [2010] "Global dynamics of the Lorenz system with invariant algebraic surfaces," *Int. J. Bifurcation and Chaos* **20**, 3137–3155.

Lorenz, E. N. [1963] "Deterministic nonperiodic flow," *J. Atmos. Sci.* **20**, 130–141.

Lü, J., Zhou, T., Chen, G. & Zhang, S. [2002] "Local bifurcations of the Chen system," *Int. J. Bifurcation and Chaos* **12**, 2257–2270.

Shilnikov, L., Turaev, D. & Chua, L. [2001] *Methods of Qualitative Theory in Nonlinear Dynamics*: *Part 2* (World Scientific, Singapore).

Sprott, J. C. [2010] *Elegant Chaos*: *Algebraically Simple Chaotic Flows* (World Scientific, Singapore).

Tigan, G. & Opriş, D. [2008] "Analysis of a 3D chaotic system," *Chaos Solit. Fract.* **36**, 1315–1319.

Ueta, T. & Chen, G. [2000] "Bifurcation analysis of Chen's equation," *Int. J. Bifurcation and Chaos* **10**, 1917–1931.